MEDSAE: DISSECTING MEDCLIP REPRESENTATIONS WITH SPARSE AUTOENCODERS

Riccardo Renzulli* Colas Lepoutre[†]

Enrico Cassano*

Marco Grangetto*

* University of Turin, Italy †École polytechnique, Palaiseau, France

ABSTRACT

Artificial intelligence in healthcare requires models that are accurate and interpretable. We advance mechanistic interpretability in medical vision by applying Medical Sparse Autoencoders (MedSAEs) to the latent space of MedCLIP, a vision-language model trained on chest radiographs and reports. To quantify interpretability, we propose an evaluation framework that combines correlation metrics, entropy analyzes, and automated neuron naming via the MedGEMMA foundation model. Experiments on the CheXpert dataset show that MedSAE neurons achieve higher monosemanticity and interpretability than raw MedCLIP features. Our findings bridge high-performing medical AI and transparency, offering a scalable step toward clinically reliable representations.

Index Terms— Medical imaging, Artificial Intelligence, Interpretability, Sparse Autoencoders

1. INTRODUCTION

The emergence of Artificial Intelligence (AI) in healthcare systems is revolutionizing the way patients are diagnosed, treated, and monitored. Deep learning models have achieved remarkable results in various medical tasks [1, 2]. As the volume of medical data continues to grow, the size and complexity of neural network architectures have also increased. Self-supervised approaches now enable these models to train on diverse data sources (e.g., text, signals, images) with minimal reliance on human annotations, leading to the development of Multimodal Large Language Models (MLLMs) [3].

Despite their advancements, MLLMs have notable limitations: they are computationally expensive and difficult to interpret. Mechanistic interpretability techniques [4] are emerging as powerful tools to reverse-engineer the computational mechanisms of neural networks into human-understandable concepts. However, scaling these techniques to MLLMs and applying them to complex medical tasks remains an open challenge. In this work, as shown in Figure 1, we present the first empirical analysis of mechanistic interpretability in medical MLLMs using Medical Sparse Autoencoders (Med-SAEs) to uncover meaningful internal representations from MedCLIP [5], trained on chest X-rays. We propose an automated feature naming via MedGEMMA [6], a foundation

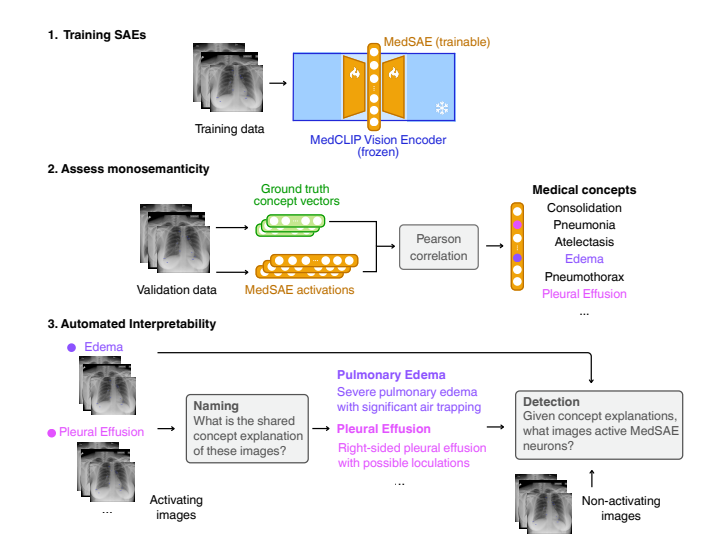


Fig. 1: The overall proposed pipeline. (1) We first train Med-SAE from MedCLIP vision encoder and extract corresponding embeddings. (2) Then, we compute their Pearson correlation with one-hot encoded vector labels to identify MedSAE neurons-concepts mappings. (3) As final step, for each Med-SAE neuron, top-activating images are used to generate concept names via structured prompting. These names are validated through a detection task, where MedGEMMA yields a quantitative measure of semantic alignment.

vision-language model that assigns and validates humaninterpretable labels to individual MedSAE neurons.

Our experiments show that MedSAE features exhibit higher class selectivity and stronger alignment with clinical concepts than those from raw MedCLIP embeddings. Notably, we identify and name 21 medically meaningful features using MedGEMMA with high interpretability accuracy.

2. BACKGROUND AND RELATED WORK

2.1. Sparse Autoencoders

Mechanistic interpretability aims to decompose deep learning models into human-understandable components by analyzing their model activations. This includes labeling circuits

and neurons using feature visualization techniques, as well as quantifying concept activations and directions within the latent space [4]. However, these efforts face challenges due to polysemantic neurons, namely neurons that respond to multiple, unrelated concepts [7]. SAEs learn to reconstruct inputs using a sparse set of features in a higher-dimensional space, potentially disentangling superposed features [4]. A standard single-layer ReLU SAE operates on d-dimensional activation vectors. Let $\mathbf{x} \in \mathbb{R}^d$ denote the input activation vector and m be the SAE latent dimension, typically set to d multiplied by a positive expansion factor. The encoder and decoder are defined as [8]:

$$\mathbf{z} = \text{ReLU}(\mathbf{W}_{enc}(\mathbf{x} - \mathbf{b}_{pre}) + \mathbf{b}_{enc})$$

$$\hat{\mathbf{x}} = \mathbf{W}_{dec}\mathbf{z} + \mathbf{b}_{pre},$$
(1)

where $\mathbf{W}_{enc} \in \mathbb{R}^{m \times d}$ and $\mathbf{W}_{dec} \in \mathbb{R}^{d \times m}$ are the encoder and decoder weight matrices respectively, and $\mathbf{b}_{pre} \in \mathbb{R}^d$ and $\mathbf{b}_{enc} \in \mathbb{R}^m$ are learnable bias terms.

To encourage sparsity in the latent representation **z**, an L1 penalty is added to the objective:

$$\mathcal{L} := \|\mathbf{x} - \hat{\mathbf{x}}\|_2^2 + \lambda \|\mathbf{z}\|_1, \tag{2}$$

where $\lambda > 0$ controls regularization strength.

2.2. Mechanistic Interpretability for Healthcare

While the literature on mechanistic interpretability in healthcare remains relatively limited, there is a growing interest in applying sparse autoencoders (SAEs) to reveal interpretable representations in medical imaging models. For instance, [9] employed SAEs to debug melanoma detection networks, uncovering dataset biases through neuron activation patterns. Similarly, [10] used SAEs to generate radiology reports by mapping image tokens into interpretable features, achieving both transparency and competitive diagnostic performance. More recently, [11] applied SAEs to vision transformers in histopathology, identifying biologically meaningful features, such as specific cell types, with improved robustness to confounding factors. A major challenge across these works lies in naming and semantically grounding the discovered features. Building on this foundation, our work further investigates SAEs in medical vision models, specifically for radiological imaging, by training a ReLU-based SAE on Med-CLIP, a vision-language model for chest X-rays, and introducing a domain-specific framework for neuron naming and interpretability evaluation.

3. METHODOLOGY

We now present our methodology for extracting and evaluating interpretable latent representations using SAEs. As illustrated in Figure 1, our MedSAE pipeline comprises three main stages: (1) training SAEs on MedCLIP embeddings, (2)

assessing neuron monosemanticity, and (3) performing automated interpretability and neuron naming. Each step is detailed in the following subsections.

3.1. Image Embeddings Extraction and Training

Images embeddings are computed using MedCLIP-ResNet. MedCLIP embeddings can exhibit misalignment across modalities, which can impact SAE training convergence and cross-modal transferability. Following [12], we normalize embeddings to ensure consistent behavior across modalities. We first center embeddings by subtracting the per-modality mean estimated from the training dataset. Next, we scale the centered embeddings by a dataset-computed scaling factor following [13] to obtain $\mathbb{E}_{\mathbf{x} \in \mathcal{X}}[\|\mathbf{x}\|_2] = \sqrt{d}$ with d the dimension of the MedCLIP embeddings. We then train ReLUbased SAEs on these normalized embeddings, encouraging sparse and disentangled activations. This scaling ensures that λ has consistent effects across different CLIP architectures and modalities.

3.2. Assessing SAEs Monosemanticity

As a first step toward validating monosemanticity and the alignment of neurons with clinically meaningful concepts, we leverage label-based correlation analyses to identify neurons that are selectively responsive to specific medical findings. Inspired by the approach in [11], we use the Pearson correlation coefficient to quantify the strength of the linear relationship between each neuron's activation and the presence or absence of a particular medical finding. Let $\mathbf{Z} \in \mathbb{R}^{n \times m}$ be the activation matrix of the SAE, where n is the number of samples and m the number of neurons. Let $\mathbf{Y} \in \mathbb{R}^{n \times k}$ be the corresponding one-hot encoded label matrix, with k the number of labels. The Pearson correlation between neuron i and label j is computed as:

$$\rho_{i,j} = \frac{\text{Cov}(\mathbf{Z}_i, \mathbf{Y}_j)}{\sigma_{\mathbf{Z}_i} \sigma_{\mathbf{Y}_j}}$$
(3)

To evaluate whether a neuron is *monosemantic* (i.e., predominantly associated with a single concept) we compute the entropy of its correlation distribution across all labels. Specifically, we define:

$$p_{i,j} = \frac{|\rho_{i,j}|}{\sum_{k} |\rho_{i,k}|} \tag{4}$$

Then, the entropy of neuron i is given by:

$$H_i = -\sum_{j} p_{i,j} \log_2 p_{i,j} \tag{5}$$

A lower entropy H_i indicates that neuron i is sharply peaked on a single concept, suggesting high monosemanticity. In contrast, higher entropy implies more distributed activation across multiple concepts. In practice, we use the

average entropy across MedSAE neurons as a selection criterion to compare different configurations and identify the model that achieves the highest degree of monosemanticity.

3.3. Automated Naming with MedGEMMA

We leverage the capabilities of MedGEMMA to generate semantic interpretations for groups of SAE activations. Given a set of X-ray images that strongly activate a particular latent feature, we prompt MedGEMMA to identify and summarize the shared concept underlying these samples. These interpretations can reflect medical phenomena (e.g., a specific pathology or anatomical abnormality) or non-medical characteristics (e.g., image artifacts, patient positioning, or device presence). This automated naming framework enables us to attach human-readable labels to otherwise abstract SAE neurons, serving as a first step toward interpretable latent representations in the medical domain.

While automated naming provides semantic anchors for SAE features, it does not inherently guarantee accuracy or clinical relevance. Therefore, we incorporate validation strategies to assess the consistency and interpretability of the generated names. To this end, we adopt the detection metric introduced by [14]. In this setup, MedGEMMA is provided with a generated interpretation and a balanced set of activating and non-activating images. It is then asked to identify which images match the concept described—effectively performing a binary classification task. This allows us to assess whether the interpretation genuinely reflects a consistent and isolatable feature in the image space.

4. EXPERIMENTS AND RESULTS

This section evaluates our previously introduced method, showing that MedSAEs effectively disentangle superposed representations in MedCLIP embeddings, revealing structured and clinically meaningful features. These results support the potential of SAEs as a practical tool for mechanistic interpretability in vision-language models, bridging the gap between deep feature representations and human-understandable medical concepts.

4.1. Dataset and implementation details

To ensure consistency with the MedCLIP data distribution, our study employed CheXpert dataset [15]. We curated a balanced evaluation dataset from CheXpert, comprising exactly 200 images per class.

We trained our ReLU-MedSAEs on the last layer of a MedCLIP-ResNet (d=512) on the original CheXpert train split for 200 epochs. We choose a learning rate of $7\cdot 10^{-6}$, a L1 penalty coefficient λ of $3\cdot 10^{-4}$ and an expansion rate of 16.

4.2. Interpretable Feature Disentanglement: Monosemanticity of SAE Neurons and Medical Class Correlations

We select the model that achieves the best neuron-class entropy on CheXpert14x200. This model also maintains a favorable sparsity–reconstruction balance, with a 0.20% L0 activation rate and a 0.98 feature variance explained (FVE) despite a significant amount of dead neurons (30%). Those results align with reasonable sparsity settings as identified by [16]. As expected, we find that neurons from the SAE exhibit lower entropy compared to MedCLIP's raw embeddings, indicating improved monosemantic behavior (2.25 vs 2.38).

4.3. Discovering Medical Concepts via MedGEMMA-Based Automated Interpretability

Our previous analyses suggest that some SAE neurons exhibit strong correlations with specific medical concepts, indicative of monosemanticity. However, while such patterns point to interpretability, they do not reveal the real semantic of each neuron. To uncover these latent concepts, we apply the MedGEMMA-Based Automated Interpretability framework introduced in Section 3.3.

We examine the individual neurons with the highest interpretation accuracy. As shown in Table 1, we identified 21 different SAE neuron interpretations with detection accuracy above 70%, in contrast to just two for MedCLIP embeddings. Many of these neurons align with clinically coherent concepts such as severe pulmonary edema, right-sided pleural effusion, or cardiomegaly with vascular congestion.

| Neuron | Accuracy | Concept Description |
|--------|----------|--|
| 1215 | 0.82 | Severe pulmonary edema with significant air trapping and subcutaneous emphysema |
| 7468 | 0.77 | Right upper lobe consolidation with possible cavitation |
| 2320 | 0.75 | Right-sided pleural effusion with possible loculations |
| 876 | 0.75 | Diffuse bilateral infiltrates with significant opacification of the lung fields, likely due to pulmonary edema or infectious process |
| 85 | 0.73 | Diffuse bilateral interstitial lung disease (ILD) with multiple lines of central venous access |
| 3826 | 0.73 | Pulmonary edema with cardiomegaly |
| 4214 | 0.73 | Severe cardiomegaly with significant pulmonary vascular congestion |
| 283 | 0.73 | Severe right-sided pneumothorax with significant subcutaneous emphy- sema and multiple lines/tubes in place |
| 817 | 0.73 | Right-sided pleural effusion with loculations |
| 1859 | 0.73 | Large left pleural effusion with possible loculation |
| 5929 | 0.73 | Diffuse bilateral pulmonary infiltrates |
| 127 | 0.72 | Pulmonary edema with significant bilateral opacities |
| 5616 | 0.72 | Normal chest X-ray with clear visualization of lungs, heart, and rib cage in upright position |
| 1251 | 0.72 | Cardiac device placement and associated pulmonary edema |
| 2378 | 0.72 | Severe bilateral pulmonary infiltrates with significant opacification of both lung fields, likely due to edema or infection |
| 2862 | 0.72 | Pulmonary edema with significant pulmonary vascular congestion and cardiomegaly |
| 8153 | 0.72 | Right-sided pleural effusion with significant underlying lung opacity |
| 4728 | 0.70 | Cardiomegaly with pulmonary edema |
| 1266 | 0.70 | Diffuse bilateral pulmonary infiltrates with central line placement |
| 2708 | 0.70 | Right-sided pleural effusion with pulmonary edema |
| 6552 | 0.70 | Normal adult chest radiograph |

Table 1: Top SAE neurons and their corresponding MedGEMMA-generated concepts, sorted by detection accuracy. Duplicate concept descriptions have been removed.

Overall, these findings provide additional evidence that the SAE architecture promotes disentanglement, giving rise to individual neurons that robustly encode specific and medically meaningful concepts.

5. CONCLUSION

This work presents a first step toward mechanistic interpretability in medical vision-language models by leveraging sparse autoencoders to extract clinically meaningful and monosemantic features from MedCLIP embeddings. Our evaluation framework, combining correlation metrics and automated neuron naming via MedGEMMA, demonstrates improved interpretability and alignment with clinical concepts on the CheXpert dataset. Despite promising results, several challenges remain, such as the presence of inactive neurons and the need for more expressive SAE architectures, the computational cost and dataset sensitivity of automated naming, and the limited validation across modalities and institutions. However, our results highlight sparse autoencoders as a promising direction for building more transparent, robust, and trustworthy medical AI systems.

Compliance with ethical standards. No ethical approval was required because of the retrospective use of open source datasets.

Acknowledgments We acknowledge the CINECA award under the ISCRA initiative, for the availability of high performance computing resources and support.

6. REFERENCES

- [1] Geert Litjens et al., "A survey on deep learning in medical image analysis," *Medical Image Analysis*, vol. 42, pp. 60–88, 2017. 1
- [2] P. Celard et al., "A survey on deep learning applied to medical images: from simple artificial neural networks to generative models," *Neural Computing and Applications*, vol. 35, no. 3, pp. 2291–2323, Jan 2023. 1
- [3] Jiayang Wu et al., "Multimodal large language models: A survey," in 2023 IEEE International Conference on Big Data (BigData), 2023, pp. 2247–2256. 1
- [4] Leonard Bereska and Stratis Gavves, "Mechanistic interpretability for AI safety a review," *Transactions on Machine Learning Research*, 2024, Survey Certification, Expert Certification. 1, 2
- [5] Zifeng Wang et al., "MedCLIP: Contrastive learning from unpaired medical images and text," in *Proceed*ings of the 2022 Conference on Empirical Methods in Natural Language Processing, Yoav Goldberg, Zornitsa Kozareva, and Yue Zhang, Eds., Abu Dhabi, United

- Arab Emirates, Dec. 2022, pp. 3876–3887, Association for Computational Linguistics. 1
- [6] Andrew Sellergren et al., "Medgemma technical report," 2025.
- [7] Nelson Elhage et al., "A mathematical framework for transformer circuits," *Transformer Circuits Thread*, 2021, https://transformercircuits.pub/2021/framework/index.html.
- [8] Trenton Bricken et al., "Towards monosemanticity: Decomposing language models with dictionary learning," Transformer Circuits Thread, 2023, https://transformer-circuits.pub/2023/monosemantic-features/index.html.
 2
- [9] Maximilian Dreyer et al., "Mechanistic understanding and validation of large AI models with SemanticLens," *Nature Machine Intelligence*, pp. 1–14, Aug. 2025, Publisher: Nature Publishing Group. 2
- [10] Ahmed Abdulaal et al., "An x-ray is worth 15 features: Sparse autoencoders for interpretable radiology report generation," 2024. 2
- [11] Nhat Minh Le et al., "Learning biologically relevant features in a pathology foundation model using sparse autoencoders," in *Advancements In Medical Foundation Models: Explainability, Robustness, Security, and Beyond*, 2024. 2
- [12] Usha Bhalla et al., "Interpreting CLIP with sparse linear concept embeddings (spliCE)," in *The Thirty-eighth Annual Conference on Neural Information Processing Systems*, 2024. 2
- [13] Tom Conerly et al., "Update on how we train saes," Transformer Circuits Thread, 2024. 2
- [14] Gonçalo Santos Paulo et al., "Automatically interpreting millions of features in large language models," in *Forty-second International Conference on Machine Learning*, 2025. 3
- [15] Jeremy Irvin et al., "Chexpert: a large chest radiograph dataset with uncertainty labels and expert comparison," in Proceedings of the Thirty-Third AAAI Conference on Artificial Intelligence and Thirty-First Innovative Applications of Artificial Intelligence Conference and Ninth AAAI Symposium on Educational Advances in Artificial Intelligence. 2019, AAAI'19/IAAI'19/EAAI'19, AAAI Press. 3
- [16] Leo Gao et al., "Scaling and evaluating sparse autoencoders," in *The Thirteenth International Conference on Learning Representations*, 2025. 3